South African Journal of Chemical Engineering 55 (2026) 63–71

Contents lists available at ScienceDirect

South African Journal of Chemical Engineering

journal homepage: www.elsevier.com/locate/sajce

Influence of carbon sources and biosurfactants on selenite and lead bioremediation by *Enterococcus* sp

Job T. Tendenedzai *, Evans M.N. Chirwa, Hendrik G. Brink

Water Utilisation and Environmental Engineering Division, Department of Chemical Engineering, University of Pretoria, 0002, South Africa

ARTICLE INFO

Keywords:
Bioprecipitation
Biosorption
Bioreduction
Glucose
Cooking oil
Crude oil

ABSTRACT

This study explored *Enterococcus* sp.'s potential for bioremediating selenite (SeO_3^{2-}) and lead (Pb^{2+}) contamination using different carbon sources (glucose, cooking oil and crude oil) while elucidating the underlying mechanisms. Aerobic batch reduction experiments were conducted (35±2 °C, 120 rpm, pH≈8, 50 h) with an initial 1 mM concentration of either SeO_3^{2-} or Pb^{2+} which was quantified by Ion Chromatography and Atomic Absorption Spectroscopy respectively. Key results showed that carbon source selection significantly influenced SeO_3^{2-} and Pb^{2+} removal rates, elemental selenium (Se^0) formation, and protein synthesis. Glucose and cooking oil were found to be the most efficient, leading to rapid SeO_3^{2-} reduction (58 % and 55 % reduction, respectively), compared to crude oil (39 %). Similarly, Pb^{2+} removal rates followed a similar trend, with 38 %, 33 %, and 25 % reduction using glucose, cooking oil, and crude oil, respectively. The study also highlighted *Enterococcus* sp.'s varied mechanisms for SeO_3^{2-} and Pb^{2+} reduction, with SeO_3^{2-} precipitating to Se^0 while no precipitation of Pb^{2+} to Pb^0 was observed. Furthermore, the bacteria exhibited versatility in biosurfactant production across the various carbon substrates. The biosurfactants notably promoted Se^0 precipitation thus shedding light on their potential role in metal ion bioreduction.

1. Introduction

Water pollution by toxic metals and metalloids remains a major environmental challenge due to their persistence, bioaccumulation, and risks to human and ecosystem health. Among these contaminants, selenium (Se) and lead (Pb) are of particular concern. Selenium, although an essential micronutrient for plants and humans, has a very narrow safety margin and therefore requires strict monitoring (Brozmanova et al., 2010; Huang et al., 2019). Anthropogenic activities such as mining, coal burning, and agriculture have elevated Se concentrations in surface waters, mainly in the form of selenate and selenite oxyanions (Mehdi et al., 2013). The recommended maximum allowable concentration of Se oxyanions in surface water is 40 $\mu g.L^{-1}$ (Brink et al., 2018). Similarly, Pb pollution from industrial and agricultural activities frequently exceeds the 10–15 $\mu g.L^{-1}$ limit in drinking water, posing severe neurological and developmental risks (Chowdhury et al., 2022). These risks necessitate effective remediation strategies.

Conventional methods for remediating metal and metalloid contamination such as chemical precipitation, adsorption, and membrane separation can be effective but are often costly, energy-intensive, and generate secondary waste. Biological approaches provide eco-friendly and sustainable alternatives, with bacterial bioremediation offering particular promise (Van Khanh Nguyen et al., 2016). Importantly, these processes can be linked to circular economy principles, where remediation is coupled with the recovery of valuable by-products (Wang et al., 2022b).

Certain metals and metalloids can be transformed into valuable nanomaterials when reduced from their ionic to elemental forms. Microorganisms facilitate this mainly through two mechanisms: (i) bioprecipitation/bioreduction, where soluble ions are enzymatically reduced to insoluble or elemental forms, and (ii) biosorption, in which ions are passively bound to cell walls, extracellular polymeric substances (EPS), or secreted biomolecules (Ayangbenro and Babalola, 2017; Pratush et al., 2018). These mechanisms are well-documented in the case of selenium and lead.

In the case of selenium, bacterial biomass has been shown to mediate selenite reduction, producing elemental selenium (Se^0), often in nanoparticle form (Tendenedzai et al., 2021). Beyond whole-cell activity, extracellular biomolecules such as EPS and cell-free extracts can also facilitate selenite reduction (Gupta and Diwan, 2017; Tendenedzai et al.,

* Corresponding author.
E-mail addresses: job.tendenedzai@tuks.co.za (J.T. Tendenedzai), evans.chirwa@up.ac.za (E.M.N. Chirwa), deon.brink@up.ac.za (H.G. Brink).

https://doi.org/10.1016/j.sajce.2025.10.008
Received 31 December 2024; Received in revised form 29 September 2025; Accepted 29 October 2025
Available online 30 October 2025

2022). Several bacterial species, including *Pseudomonas stutzeri* and *Bacillus subtilis*, are reported to convert selenite into selenium nanoparticles through enzymatic pathways (Jia et al., 2022). These findings emphasize the importance of both cell-associated and extracellular processes in selenium detoxification and nanoparticle biosynthesis.

For lead, bacterial biomass has also been shown to contribute significantly to bioremediation. While some studies suggest limited evidence for enzymatic Pb^{2+} reduction to elemental Pb^0, biosorption plays a dominant role (Cilliers et al., 2022). Lead ions readily bind to bacterial cell walls, EPS, and secreted biomolecules, enabling their removal from solution without requiring enzymatic reduction (Gabr et al., 2008; Naik and Dubey, 2013). Various bacterial genera such as *Bacillus, Microbacterium*, and *Pseudomonas* have been reported to biosorb lead, cadmium, and nickel ions (Long et al., 2021). This highlights biosorption as a rapid and versatile mechanism for mitigating Pb toxicity.

Surfactants are surface-active compounds that lower surface and interfacial tension, functioning as emulsifiers, detergents, wetting agents, or dispersants (Gidudu and Chirwa, 2022). Biosurfactants (BS) are their microbial equivalents, produced mainly as extracellular polymeric substances (EPS), and are valued for their biodegradability, low toxicity, and effectiveness in diverse environments. Owing to these properties, BS have been widely explored for the remediation of organic pollutants, including petroleum hydrocarbons (Rizvi et al., 2021), where they enhance contaminant solubility, increase bioavailability, and accelerate biodegradation (Mulligan, 2021; Sharma et al., 2022). However, despite their promise, the role of BS in metal and metalloid bioreduction and in the stabilisation of biogenic nanomaterials remains underexplored (da Silva et al., 2023). This creates a critical knowledge gap in understanding how BS contribute to elemental precipitation, biosorption, and nanoparticle stabilisation under different metabolic conditions.

Addressing this gap is particularly relevant within the framework of the United Nations Sustainable Development Goals (SDGs), which emphasise clean water (SDG 6), sustainable industry and innovation (SDG 9), and protection of aquatic ecosystems (SDG 14) (Georgeson and Maslin, 2018). By advancing eco-friendly remediation strategies that not only detoxify pollutants but also recover valuable nanomaterials, BS-assisted microbial bioremediation offers a pathway toward sustainable water management and circular economy practices.

In this study, we investigated the growth and bioremediation potential of *Enterococcus* sp. against SeO_3^{2-} and Pb^{2+}, under different carbon sources (glucose, cooking oil, and crude oil), with a focus on biosurfactant production and its mechanistic involvement. Particular attention was given to the potential for Se bioprecipitation to Se^0, Pb biosorption, and the role of BS in mediating these transformations. By linking carbon source utilisation with microbial adaptability, contaminant reduction, and BS activity, this work addresses the identified knowledge gap and advances sustainable strategies for wastewater treatment and resource recovery.

2. Materials and methods

All chemicals used were from Sigma-Aldrich (St. Louis, MO, USA) unless otherwise specified.

2.1. Bacteria strain and culture conditions

The bacterial cultures utilised in this study were *Enterococcus* sp., which were isolated from a Se-laden medium obtained from a laboratory at the University of Pretoria, South Africa. The characterisation and identification of the bacteria were performed using TEM, SEM, and 16S rRNA sequencing, with the latter outsourced to Inqaba Biotechnical Industries (Pty) Ltd (Tendenedzai et al., 2021). For cultivation and storage, the *Enterococcus* sp. was cultured in Tryptone Soy Broth (TSB) for 24 h at 28 °C on a rotary shaker operating at 120 rpm (FSIM-SPO8, Labcon, Johannesburg, South Africa). After 24 h, 0.8 mL of the TSB containing the bacteria was transferred to sterilised 2 mL vials, followed by the addition of 0.2 mL of a 50 % glycerol solution. These vials were then placed in a freezer at −70 °C. To revive the bacterial strain, the frozen vials were removed from the freezer, and loops were used to streak the contents of the vials onto agar plates.

2.2. Experimental design

The experiment was designed to assess the influence of carbon source on the ability of *Enterococcus* sp. to reduce selenite (as Na_2SeO_3) and lead (as $Pb(NO_3)_2$) under aerobic batch conditions. The workflow included inoculum preparation, batch reactor setup, contaminant analysis, and protein quantification, with appropriate controls to differentiate biological from abiotic processes.

Agar plates were prepared and streaked with *Enterococcus* sp. and incubated overnight at 35 °C. After 24 h, well-isolated colonies were transferred into Tryptone Soy Broth (TSB) and incubated at 35 °C and 120 rpm for an additional 24 h to generate actively growing inocula.

Three sets of mineral salts medium (MSM), prepared according to (Tendenedzai et al., 2021), were amended with either selenite or lead at an initial concentration of 1 mM (173 ppm SeO_3^{2-}; 207 ppm Pb^{2+}). Each set was further supplemented with one of three carbon sources: glucose, cooking oil, or crude oil (1 % w/v). After sterilisation, 100 mL of MSM was transferred into sterile 250 mL Erlenmeyer flasks and inoculated with 10 mL of the 24 h broth culture. Flasks were incubated under shaking conditions (35 ± 2 °C, 120 rpm, initial pH 8.0 ± 0.2) for 50 h. Sampling was done at specific intervals and at each interval, 5 mL of culture was aseptically withdrawn and separated into supernatant and pellet fractions for subsequent analysis.

2.3. Analytical methods

The concentration of aqueous selenite (SeO_3^{2-}) was quantified using ion chromatography (940 Professional IC Vario, Metrohm, Herisau, Switzerland) equipped with a Metrosep C 6–250/4.0 separation column and operated with an 8 mM oxalic acid eluent at a flow rate of 0.7 mL min^{-1}. Samples were first centrifuged at 6 000 rpm for 10 min and filtered through 0.22 μm syringe filters to remove residual biomass.

The recovery of elemental selenium (Se^0) was determined following acid digestion of the cell pellet according to Tendenedzai et al. (2023). Briefly, pellets collected by centrifugation (6 000 rpm, 10 min) were rinsed with deionised water and comprised both Se^0 and bacterial biomass. The combined pellet was acidified with 2 mL of concentrated nitric acid (70 %) and hydrochloric acid (32 %) in a 3:1 ratio (aqua regia) and digested in a thermoreactor at 100 °C for 60 min to ensure complete dissolution and re-oxidation of Se^0. The digested samples were cooled, diluted with deionised water, and analysed using flame atomic absorption spectroscopy (AAS; PerkinElmer AAnalyst 400, Waltham, MS, USA) at a wavelength of 196.0 nm.

The residual aqueous Pb^{2+} concentration in the supernatant was quantified using the same AAS instrument fitted with a Pb Lumina hollow cathode lamp (Cilliers et al., 2020). For Pb associated with the pellet fraction, digestion was carried out by adding 0.1 mL of 55 % nitric acid (Glassworld, Johannesburg, South Africa) and 0.1 mL of distilled water. After complete dissolution, the sample was diluted to a final volume of 1 mL with deionised water and analysed by AAS for Pb content (Cilliers et al., 2020).

Protein concentration was determined using the Bradford assay, which relies on the binding of Coomassie dye to protein molecules under acidic conditions, producing a colour shift from brown to blue (Bradford, 1976; Tendenedzai et al., 2021). This interaction shifts the dye's absorption maximum from 465 to 595 nm, with the increase in absorbance at 595 nm serving as the quantitative measure of protein content. In this study, 0.05 mL of each standard or unknown sample was transferred into appropriately labelled cuvettes, followed by the addition of 1.5 mL of Coomassie Plus Reagent. The mixtures were incubated

for 10 min at room temperature, and absorbance was measured at 595 nm using a spectrophotometer (WPA, Light Wave II, Labotech, South Africa) zeroed against a reagent blank prepared with deionised water.

For biosurfactant production, bacterial broth was inoculated into a modified MSM supplemented with glucose, cooking oil, or crude oil as substrate, and incubated for 5 days at 30 °C, 200 rpm, and pH 8. Extraction was performed using a chloroform–methanol solution, following Chirwa et al. (2017).

Biosurfactant activity was evaluated using multiple assays. The haemolysis test was conducted on blood agar plates after 48 h incubation at 37 °C, where clear zones around colonies indicated biosurfactant production. The drop collapse test was performed by placing 10 μL of cell-free supernatant onto an oil-coated Petri dish surface; rapid collapse of the droplet indicated reduced surface tension and thus the presence of biosurfactants (Korayem et al., 2015).

Oil displacement activity was assessed by adding 10 μL of supernatant to the centre of an oil film layered over water in a Petri dish, and the diameter of the clear zone formed was recorded as a measure of surfactant activity (Mouafi et al., 2016). Emulsification index was determined by vortexing the cell-free supernatant with crude oil and measuring the emulsified layer height (Abiodun et al., 2019). Fourier Transform Infrared (FTIR) spectroscopy was used for biosurfactant characterisation with a Perkin Elmer 1600 FTIR instrument fitted with an Attenuated Total Reflectance (ATR) crystal accessory (Perkin Elmer, Connecticut, USA).

All experiments were performed in triplicate with appropriate abiotic controls (samples without bacteria or carbon sources). A summary of experimental runs, treatments, and analytical methods is presented in Table 1.

3. Results and discussion

3.1. Screening of enterococcus sp. for biosurfactant production

Enterococcus sp., possessing haemolysins were able to discolour the blood agar in the vicinity of their colonies, thereby demonstrating alpha haemolysis. Although the bacteria tested positive for haemolytic activity regardless of the carbon source, there were differences in the haemolytic zones. The average zones were 2.9 ± 0.4 mm, 2.3 ± 0.2 mm and 0.9 ± 03 mm for the glucose, cooking oil and crude oil, respectively.

To further verify the presence of biosurfactants, the drop collapse method was used. When the cell-free supernatant was placed on the mineral oil-coated petri dish, the drop exhibited a distinctive behaviour by rapidly collapsing on the oil surface within the 1 min observation period. This collapse is a characteristic response associated with the presence of biosurfactants, indicating their successful surfactant activity in reducing the surface tension of the liquid drop and promoting its interaction with the oil (Silva et al., 2021). The presence of a clear zone in the oil displacement test indicated the successful displacement of oil by biosurfactants. This was evident across all the carbon sources.

Lastly, the emulsification index test was performed. To determine the optimal conditions of strains growth and biosurfactant production by *Enterococcus* sp., the impact of different carbon sources was assessed, and the results as shown in Fig. 1(a). After 7 d of incubation, the highest growth (OD600: 6.3) was observed in the medium containing glucose, followed by cooking oil (OD600: 5.514). The highest growth in the crude oil -containing medium appeared on day 5 (OD600: 2.617) and then began to decay.

According to the previous studies, glucose is indeed a preferred carbon source for many species of *Enterococcus* for growth, which was consistent with this study. This is because glucose is a simple sugar that can be easily metabolised (Ozyurek and Bilkay, 2017). It was found in this study that the cell-free supernatant produced using glucose as a carbon source had optimal emulsifying activity (Fig. 1(b)).

Glucose had the highest emulsifying index (EI) of 94 % followed by cooking oil (78 %) and lastly crude oil (44 %). Taken together, the higher growth and EI in glucose align with the view that substrate bioavailability governs biosurfactant yields (Aslam et al., 2023). The lower response on crude oil is expected for complex hydrophobic mixtures that require emulsification to become accessible (Nikolova and Gutierrez, 2021). These differences justify using glucose for downstream biosurfactant-assisted tests.

Therefore, glucose-based medium was selected for biosurfactant production and for the reduction of SeO_3^{2-} and Pb^{2+}in well plates. In the experiment, a well-plate-based approach was employed to investigate the SeO_3^{2-} and Pb^{2+} reducing ability of the biosurfactant (BS) with varying concentrations of the latter.

The concentrations added to the wells were 0 $g.L^{-1}$ (control), 0.25 $g.L^{-1}$, 0.5 $g.L^{-1}$, and 1 $g.L^{-1}$ of BS and 0.5 mM SeO_3^{2-}/Pb^{2+} subsequently added in each of them. The set up was left to stand at room temperature. After 24 h, the wells with BS and SeO_3^{2-} had turned darker as shown in Fig. 2(a). This was an indication of the SeO_3^{2-} reduction to Se^0. The control well remained unchanged. Notably, as the biosurfactant concentration increased within the wells, the darker (red) colour was more pronounced indicating a higher reduction. In a study on SeO_3^{2-} reduction by *Bacillus paramycoides* SP3, the authors found that biosurfactants produced by the bacterium played a role in the reduction process. They hypothesised that the biosurfactants helped to solubilise SeO_3^{2-} and facilitate its reduction as well as to stabilise the nanoparticles (Borah et al., 2021).

On the contrary, the wells with BS and Pb^{2+} remained relatively unchanged even with increase in BS concentration in Fig. 2(b). This was likely an indication that the biosurfactants either do not reduce lead or rather they cannot precipitate it into its elemental form which has a dark colouration. The lack of colour change for Pb mirrors observations that lead removal is typically via biosorption rather than reduction to Pb^0 (Cilliers et al., 2020).

These contrasting behaviours indicate substrate-specific roles of biosurfactants: they facilitate Se precipitation but do not drive Pb reduction. This supports a Se bioprecipitation pathway versus Pb biosorption under our conditions.

Table 1
Summary of experimental conditions, sample types, and analytical methods used.

Parameter measured	Sample type	Analytical method / Instrument
Aqueous selenite (SeO32-)	Supernatant	Ion chromatography (940 Professional IC Vario, Metrohm) with Metrosep C 6–250/4.0 column; 8 mM oxalic acid eluent, 0.7 mL min^{-1}
Elemental selenium (Se0)	Pellet (Se0 + biomass)	Acid digestion in aqua regia (HNO_3:HCl, 3:1) at 100 °C, 60 min; analysed by flame AAS (PerkinElmer AAnalyst 400, λ = 196.0 nm)
Aqueous Pb^{2+}	Supernatant	Flame AAS (PerkinElmer AAnalyst 400) with Pb Lumina hollow cathode lamp
Pellet-associated Pb	Pellet (Pb + biomass)	Digestion in 0.1 mL 55 % HNO_3 + 0.1 mL H_2O; diluted to 1 mL; analysed by flame AAS (PerkinElmer AAnalyst 400)
Protein concentration	Whole culture (cell-free supernatant)	Bradford assay, absorbance at 595 nm (WPA Light Wave II spectrophotometer)
Biosurfactant production	Culture supernatant / plates	Haemolysis, drop collapse, oil displacement, emulsification index; FTIR characterisation (Perkin Elmer 1600 FTIR, ATR accessory)

3.2. Biosurfactant characterisation

Lactic acid bacteria, including *Enterococcus* sp. (*E. faecalis* and *E. faecium*), are known to produce diverse biosurfactants with applications in pharmaceuticals, beverages, preservatives, and environmental remediation (Gayathiri et al., 2024). The type of carbon source affects biosurfactant production. Common carbon sources are vegetable oils (e.

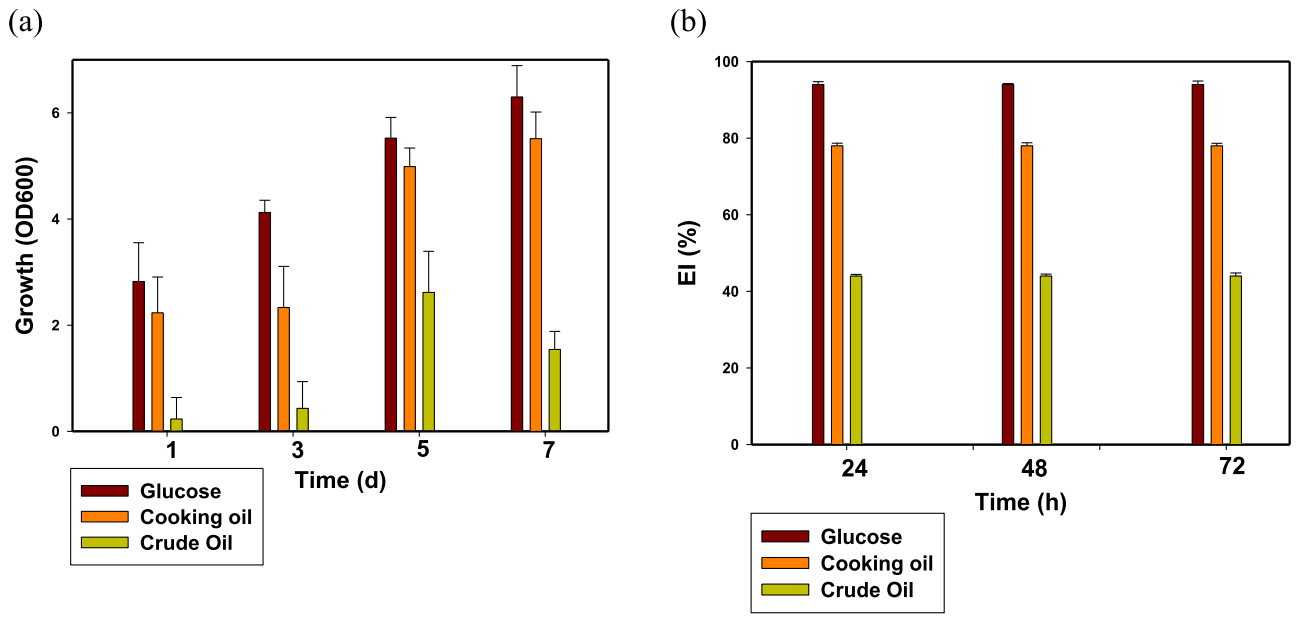

Fig. 1. The growth (a) and emulsifying indexes (b) of Enterococcus sp. in different carbon sources.

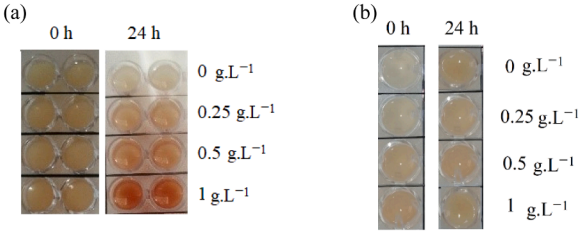

Fig. 2. (a) SeO_3^{2-} and (b) Pb^{2+} colour change with increase in biosurfactant concentration.

g., sunflower, soybean, olive oil), hydrocarbons (like n-hexadecane, n-hexane, octadecane), and carbohydrates (e.g., glucose, sucrose, fructose, mannitol, lactose) (Aslam et al., 2023).

In this study, glucose, cooking oil, and crude oil were used as carbon sources for *Enterococcus* sp. FTIR analysis was conducted to determine differences in the biosurfactants produced. The results from the analyses indicate that the functional groups on the biosurfactants were largely similar regardless of the carbon source in use and they are summarised in Table 2. The exception was with crude oil produced biosurfactant which did not have certain peaks as indicated in Fig. 3.

Table 2
Wavenumbers of the main bands in the FTIR spectrum of the biosurfactants.

Wavenumber (cm^{-1})	Functional groups	Reference
3310	N–H stretching group, primary or secondary amines	(Essghaier et al., 2023)
2925.6	C—H, C—H_2 stretch, Alkanes, aliphatic groups, fatty acid aliphatic chains	(Piacenza et al., 2021)
2855	C-H stretching, alkane (aliphatic stretching)	(Essghaier et al., 2023)
1745	strong C\dbondO stretching, ester	(Essghaier et al., 2023)
1642.3	strong C\dbondC stretch, monosubstituted alkene or an CO–N stretch	(Chaurasia et al., 2022; Essghaier et al., 2023)
1548	strong N—O stretching, nitro compound	(Tugarova et al., 2018)
1244	–CH3, –CH2– aliphatic chains (in proteins, lipids etc.)	(Joshi et al., 2016; Kamnev et al., 2008)
1167	C-O stretching, aliphatic ether	(Essghaier et al., 2023)

The FTIR spectra of the biosurfactants produced in the presence of the different carbon sources reveal distinct peaks at specific wavenumbers, each providing insights into the associated functional groups and their likely sources. A prominent peak at 3310 cm^{-1} corresponds to the N—H stretching group, indicating the presence of primary or secondary amines. This suggests the existence of amino-containing compounds (Essghaier et al., 2023).

Another notable peak is observed at 2925.6 cm^{-1}, signifying the stretching vibrations of carbon-hydrogen (C—H) bonds in alkanes, aliphatic groups, and fatty acid aliphatic chains. This peak indicates the presence of hydrocarbon-based compounds or organic molecules with extended hydrocarbon chains, potentially originating from lipids and proteins (Piacenza et al., 2021). At 2855 cm^{-1}, a peak is associated with C—H stretching, specifically in alkanes and the likely presence of aliphatic compounds in the biosurfactants (Essghaier et al., 2023).

A strong peak at 1745 cm^{-1} corresponds to the $C = O$ stretching, indicative of ester functional groups. The wavenumber 1642.3 cm^{-1} exhibits a strong peak, associated with $C = C$ stretching in monosubstituted alkenes or a CO—N stretch. This may indicate the presence

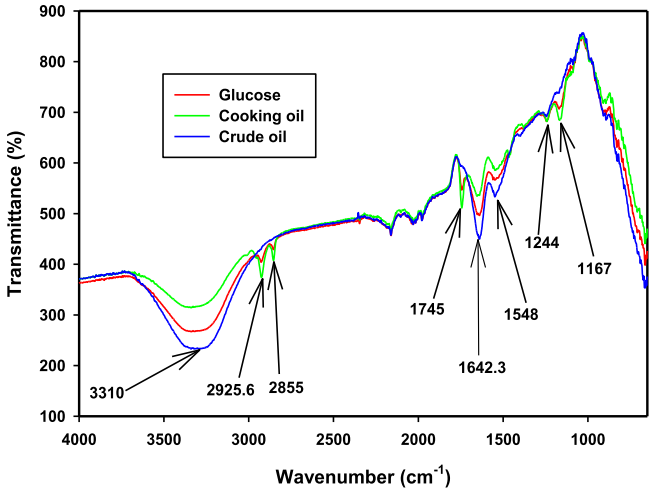

Fig. 3. FTIR spectrum of biosurfactants produced using different carbon sources.

of unsaturated compounds or other functional groups in the biosurfactants (Chaurasia et al., 2022; Essghaier et al., 2023). At 1548 cm^{-1}, a strong peak is observed, suggesting N—O stretching indicative of nitro compounds. This peak indicates the potential presence of nitro groups in the biosurfactants (Tugarova et al., 2018). The presence of methyl (-CH3) and methylene (-CH2-) groups is indicated by a peak at 1244 cm^{-1}.These aliphatic chains are commonly found in proteins, lipids, and other biomolecules (Joshi et al., 2016; Kamnev et al., 2008). A peak at 1167 cm^{-1}corresponds to C—O stretching, suggestive of aliphatic ether functional groups (Essghaier et al., 2023).

The shared functional groups across substrates suggest broadly similar biosurfactant chemistries, while attenuated peaks in the crude-oil condition point to lower yields or compositional shifts. These features are compatible with lipopeptidic or emulsifying materials that can stabilise Se^0 particulates.

3.3. SeO_3^{2-} and Pb^{2+} reduction during bacterial growth

Fig. 4(a) illustrates selenite reduction trends. *Enterococcus* sp. exhibited dual responses with glucose as the carbon source, initially rapidly reducing SeO_3^{2-} from 1 mM at time 0 h to 0.411 mM at 50 h (59 % reduction). Cooking oil showed a similar trend to glucose but with slight differences, starting reduction at 8 h and reaching 0.445 mM at 50 h (56 % reduction). Crude oil displayed a distinct pattern, with no significant reduction for the first 16 h and a final concentration of 0.603 mM at 50 h (39 % reduction). These trends are in line with Tendenedzai et al. (2023), who showed faster *Enterococcus*-mediated selenite reduction with readily metabolised donors such as glucose.

Fig. 4(b) shows elemental selenium formation. Glucose supported gradual Se^0 formation, with no measurable formation at 0 h, but steadily accumulating to 0.552 mM at 50 h. Cooking oil exhibited a similar pattern, with no initial formation at 0 h, but increasing steadily to 0.519 mM at 50 h. Crude oil supported slow but significant Se^0 formation, reaching a peak of 0.379 mM at 46 h and stabilizing thereafter. The progressive Se^0 accumulation and extracellular localisation align with prior *Enterococcus faecalis* (Shoeibi and Mashreghi, 2017) and *Azospirillum brasilense* (Tugarova et al., 2020) observations. The growth-coupled rise in Se^0 and stable recovery are consistent with extracellular nucleation followed by ripening or stabilisation of SeNPs (Yadav et al., 2023). This aligns with the biosurfactant FTIR signatures supporting nanoparticle stabilisation.

A total selenium balance was done across the different carbon sources, i.e. the measured concentrations of SeO_3^{2-}, Se^0 and the calculated total selenium in mM. The selenium accountability for glucose, cooking oil, and crude oil was 96 %, 96 %, and 98 %, respectively. These high recovery rates indicated reliability in both SeO_3^{2-} measurement and Se^0 recovery methods. Marginal differences observed suggest minor experimental errors during measurement and digestion. The high selenium mass balance argues against volatile losses, contrasting with volatilisation observed in other systems (Kagami et al., 2013). This supports

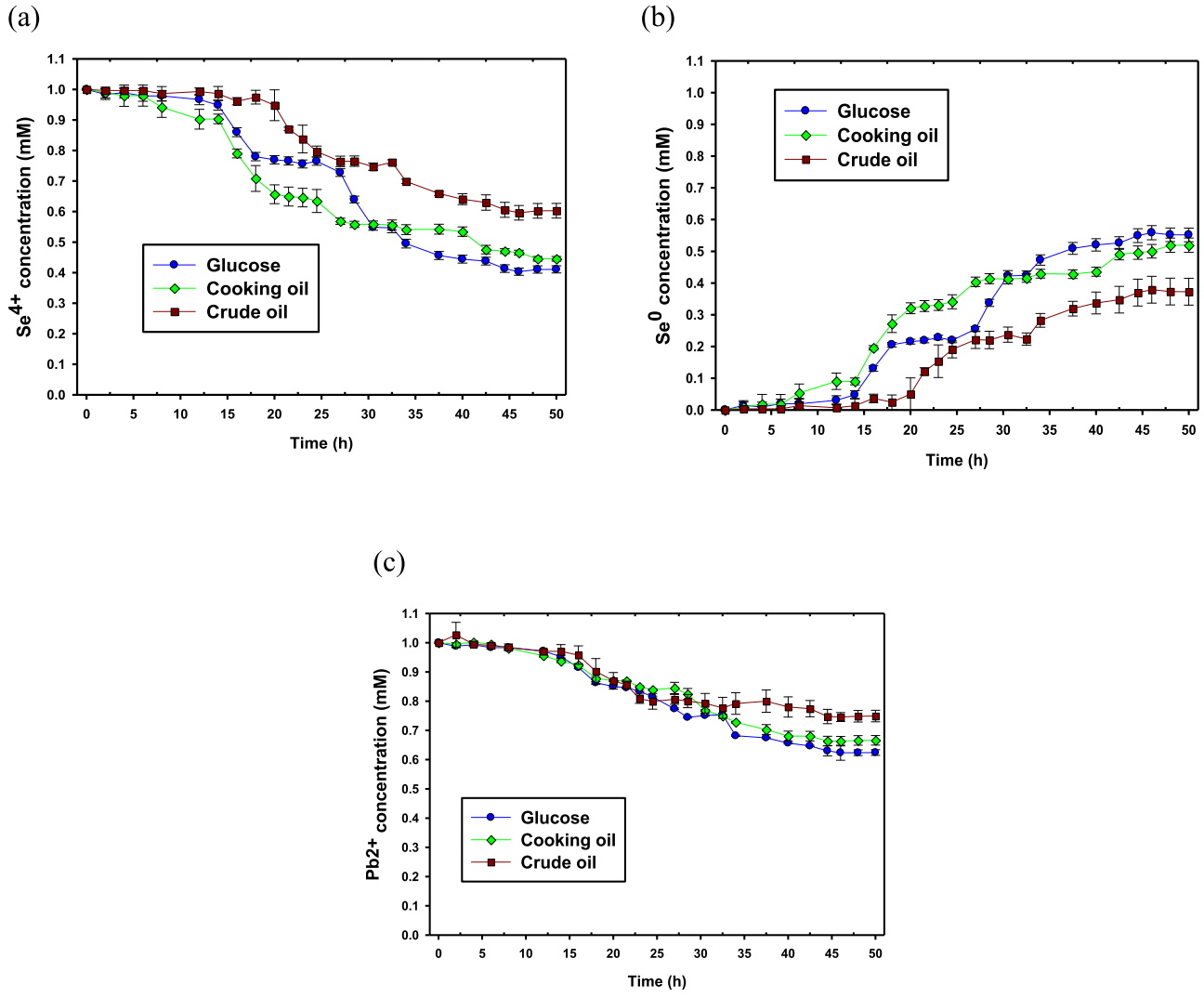

Fig. 4. (a) SeO_3^{2-} reduction and (b) Se^0 formation and (c) Pb^{2+} reduction with various carbon sources.

a dominant precipitation pathway in the aerobic reactors used in this study.

Fig. 4(c) illustrates Pb^{2+} reduction trends. Using glucose as the carbon source, Pb^{2+} concentration steadily decreased to 0.624 mM at 50 h (approximately 38 % reduction). Cooking oil showed similar trends to glucose, reducing Pb^{2+} concentration gradually to 0.666 mM at 50 h, albeit with a slightly lower reduction rate (33 % reduction). Pb^{2+} reduction with crude oil was the slowest and least efficient, with only a 25 % reduction, leaving 0.749 mM Pb^{2+} at 50 h. The steady declines without visible Pb^0 are concordant with biosorption-dominated removal rather than elemental precipitation (Cilliers et al., 2020; Naik and Dubey, 2013). Moreover, the slower kinetics on oil substrates likely reflect reduced substrate bioavailability and weaker cell activity relative to glucose. These outcomes support cell-surface binding/complexation as the operative mechanism under the prevailing conditions.

3.4. Protein synthesis

The protein production remained low during the first 6 h for SeO_3^{2-} reduction but then increased significantly, reaching a peak of 2.243×10^{-3} g.L^{-1} at 50 h with glucose as the carbon source (Fig. 5(a)). The protein content was not used only as an indicator of the likely metabolites produced by the bacteria but also as a proxy indicator for the growth and viability of the bacteria throughout the reduction of selenite. The rise in protein alongside Se reduction is consistent with protein levels tracking viability or metabolic activity under metal stress (Zheng et al., 2014).

The substantial increase in protein production suggested that glucose also promotes robust protein synthesis. In the presence of cooking oil, protein production also began around the 8 h mark with a maximum protein concentration of 2.513×10^{-3} g.L^{-1} at end of the run. Crude oil appeared to delay its support for selenite reduction and protein production, suggesting that the bacteria may require a longer adaptation period for metabolization. Protein production increased gradually, reaching a peak of 1.115×10^{-3} g.L^{-1} at 50 h. Higher protein with glucose and cooking oil indicates better energy flux and biosynthetic capacity, aligning with the faster SeO_3^{2-} removal and higher biosurfactant production as already shown in Section 3.1.

Fig. 5(b) shows the trend in protein production but, for Pb^{2+} reduction. A similar trend was observed as for selenite with the major difference being in the amount of protein detected. The amount of protein measured at 50 h was 1.046×10^{-3} g.L^{-1}, 9.532×10^{-4} g.L^{-1} and 5.469×10^{-4} g.L^{-1} for glucose, cooking oil and crude oil respectively. The lower protein concertation in Pb versus that in Se mirrors a slower metabolic response during Pb biosorption (energy-independent binding) reported in the literature (Ayangbenro and Babalola, 2017).

Overall, crude oil can ultimately serve as a carbon source for both selenite and lead reduction and protein synthesis, but the response is delayed compared to glucose and cooking oil. Crude oil is a complex mixture of hydrocarbons and other organic compounds, which makes it a difficult carbon source for bacteria to metabolise compared to simpler substances like glucose or cooking oil (Nikolova and Gutierrez, 2021). In contrast, glucose is easier to metabolise providing a readily available source of energy and carbon for metabolic processes. Similarly, cooking oil, although composed of a mixture of fatty acids and lipids, is easier to metabolise relative to crude oil (Kachienga, 2020).

The recalcitrance of oil-based substrates for *Enterococcus* sp. in metal reduction and thus their availability to the microorganism is also related to their solubility in water. This affects the accessibility of the substrate to the microorganisms and can affect the reduction process (Melati et al., 2019). Being highly soluble in water, glucose can serve as a readily available carbon source for *Enterococcus* sp., promoting their growth and metabolic activities (Tendenedzai et al., 2023). On the other hand, due to their poor solubility in water, crude oil and cooking oil are not readily accessible carbon sources for *Enterococcus* sp. The hydrophobic nature of these oils makes them less available for uptake by the bacteria, potentially limiting their growth and metabolic processes (García-Solache and Rice, 2019). This has an impact on the uptake mechanisms by the bacteria. However, *Enterococcus* sp., can utilise hydrocarbons from cooking oil and crude oil as carbon sources through mechanisms such as biosurfactant production and emulsification, which enhance the bioavailability of these substrates (Sharma et al., 2015).

3.5. *Enterococcus sp.'s* SeO_3^{2-} *and* Pb^{2+} *bioremediation mechanisms*

Microorganisms can transform heavy metals and non-metals using different mechanisms. During this transformation, the ionic state of the metal or non-metal changes and thus may affect the species' bioavailability, solubility, and mobility (Pratush et al., 2018).

In this study, *Enterococcus* sp. was found to employ distinct pathways for SeO_3^{2-} and Pb^{2+} reduction. As shown in Fig. 6(a), visible precipitation of red Se^0 confirmed an extracellular reduction process. In contrast, no Pb^0 precipitate was observed (Fig. 6(b)), even though Pb^{2+} concentrations decreased in solution, suggesting that removal occurred mainly through biosorption onto cell surfaces and extracellular biomolecules.

These findings indicate that *Enterococcus* sp. reduces SeO_3^{2-} primarily through bioprecipitation, while Pb^{2+} is sequestered via biosorption, in agreement with earlier reports Cilliers et al. (2022). The following subsections, supported by Figs. 7 and 8, describe the proposed mechanisms for SeO_3^{2-} bioprecipitation and Pb^{2+} biosorption in detail.

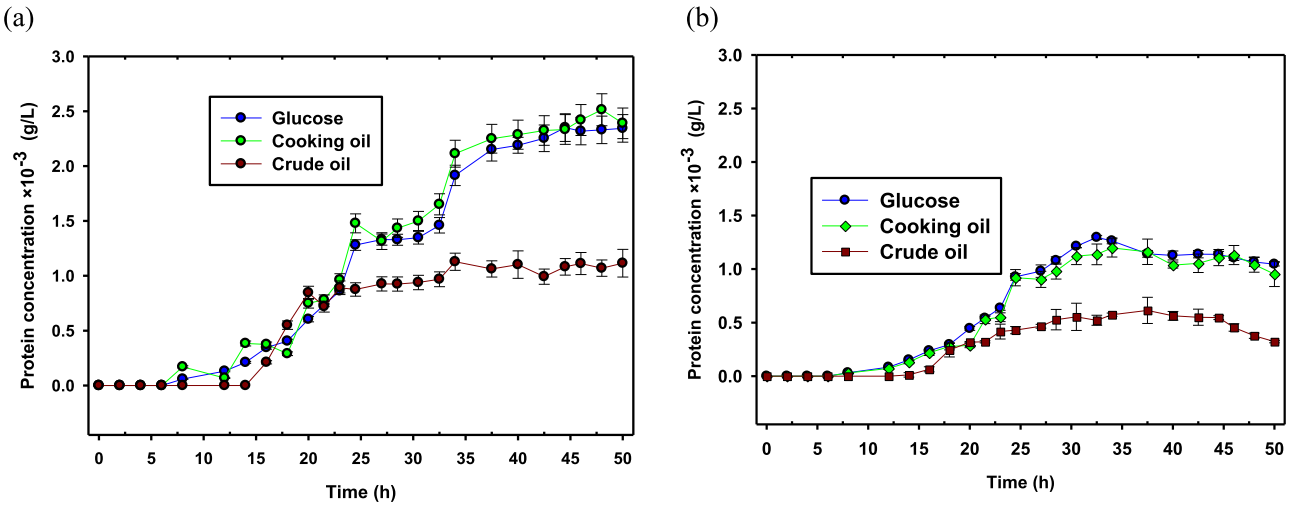

Fig. 5. Protein concentration with different carbon sources during (a) SeO_3^{2-} and (b) Pb^{2+} reduction.

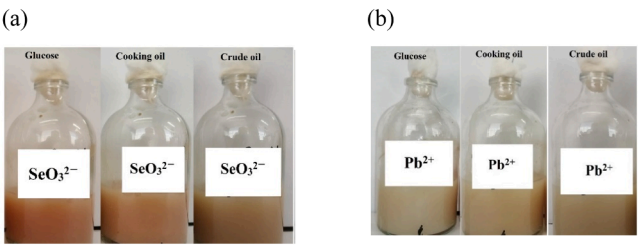

Fig. 6. SeO_3^{2-} and Pb^{2+} reduction with different carbon sources after 50 h.

3.5.1. SeO_3^{2-} bioprecipitation

Experimental results confirmed that *Enterococcus* sp. reduced SeO_3^{2-} to elemental Se^0 via bioprecipitation, with visible red Se^0 particles forming in the medium (Fig. 6(a)). This indicates that selenium removal proceeded predominantly through extracellular reduction and precipitation rather than intracellular accumulation.

Bioprecipitation is a metabolism-associated process in which soluble oxyanions are enzymatically reduced to insoluble or elemental forms, often serving as a bacterial detoxification strategy (Sreedevi et al., 2022). In this study, Se^0 nanoparticles appeared mainly outside the cells, suggesting an extracellular reduction pathway. Similar extracellular nanoparticle formation has been reported in other bacteria, such as *Enterococcus faecalis* (Shoeibi and Mashreghi, 2017).

Several mechanisms may contribute to this process. Bacterial secretions such as EPS and biosurfactants can facilitate SeO_3^{2-} reduction, stabilising the resulting Se^0 nanoparticles and promoting their aggregation via Ostwald ripening (Shahabadi et al., 2023; Yadav et al., 2023). Transcriptomic studies in other organisms have shown that enzymes

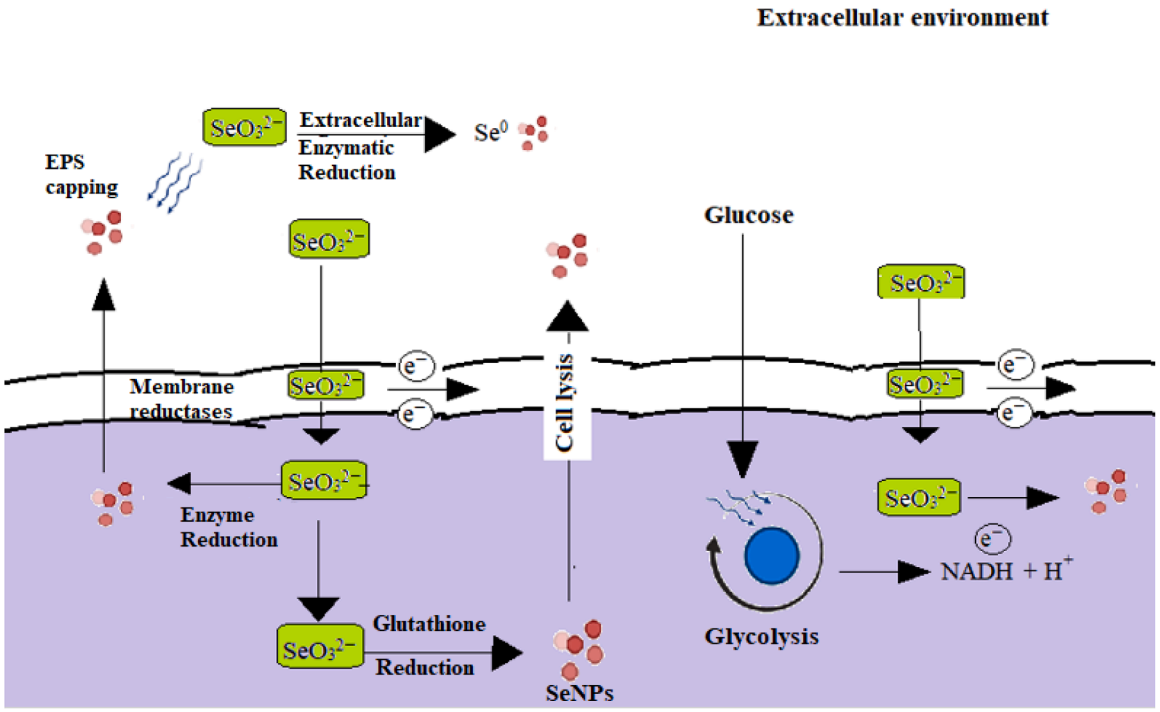

Fig. 7. Mechanism for Se^0 formation (bioprecipitation) by Enterococcus sp.

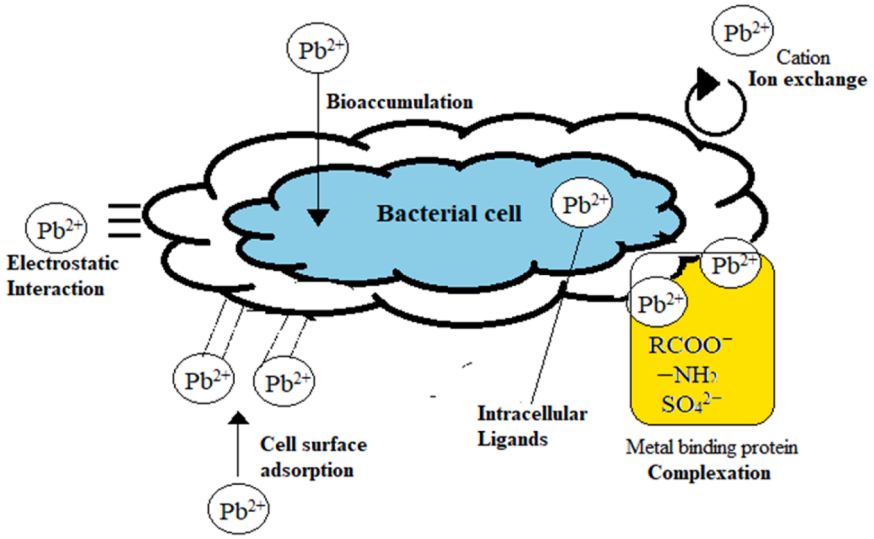

Fig. 8. Mechanism for Pb^{2+} biosorption by Enterococcus sp.

such as PutC, GabD, and CysJI reductase systems play a role in SeO_3^{2-}reduction, with Se^0 nanoparticles secreted outside the cell through membrane transport systems (Tugarova et al., 2020). Alternative pathways may involve cell lysis, releasing Se^0 particles into the extracellular environment (Jia et al., 2022; Nancharaiah and Lens, 2015).

In the presence of carbon sources such as glucose, SeO_3^{2-}reduction is closely linked to energy metabolism. Glucose metabolism via glycolysis generates nicotinamide adenine dinucleotide (NADH), which acts as an electron donor for selenite reductases, catalysing the reduction of $SeO_3^{2-}$to Se^0 (Kessi et al., 1999; Wang et al., 2022a). The resulting Se^0 aggregates into nanoparticles that are stabilised by organic coatings from EPS and biosurfactants, preventing further oxidation or aggregation.

Overall, the findings indicate that *Enterococcus* sp. removes selenium primarily through extracellular bioprecipitation, with EPS and biosurfactants enhancing Se^0 nanoparticle formation and stability as shown in Fig. 7. This mechanism not only detoxifies SeO_3^{2-}but also generates nanoscale selenium with potential applications in agriculture, medicine, and electronics.

3.5.2. Pb^{2+} biosorption

As shown in Fig. 8, Pb^{2+} reduction by *Enterococcus* sp. proceeded via biosorption rather than bioprecipitation, consistent with the absence of Pb^0 precipitate in our experiments. This indicates that Pb^{2+} removal was mediated mainly by surface interactions with bacterial cells and extracellular biomolecules, rather than enzymatic reduction.

Biosorption is generally a rapid, passive process that can occur in both live and dead cells, typically reaching equilibrium within a short time (Ayangbenro and Babalola, 2017; Hassan et al., 2010). It involves ion exchange and physical adsorption at negatively charged sites on bacterial cell walls (Fomina and Gadd, 2014). In *Enterococcus* sp., these sites may include carboxylate, phosphate, and amino groups, as well as residues within extracellular polymeric substances (EPS) such as polysaccharides and proteins (García-Solache and Rice, 2019).

Literature supports the importance of such functional groups in Pb^{2+} and other metal biosorption. For instance, *Pseudomonas aeruginosa* cell walls contain carboxylate, phosphate, and amino groups that strongly bind Pb and Ni (Gabr et al., 2008). Amino acids such as histidine, cysteine, and glutamic acid have also been implicated in metal binding ((Hassan et al., 2010; Sajadi, 2010). Similarly, EPS components facilitate complex formation with metal ions, producing mononuclear or polynuclear complexes depending on ligand availability (Sun et al., 2014).

Ion exchange is another significant pathway, where protons (H^+) or other cations are displaced by Pb^{2+} at cell wall binding sites. This process depends on ligand strength and the nature of the functional groups present. Electrostatic interactions further enhance binding, as Pb^{2+} and other highly charged cations are strongly attracted to negatively charged bacterial surfaces and EPS (Lodeiro et al., 2007; Torres, 2020).

Taken together, these mechanisms explain why Pb^{2+}concentrations decreased in the aqueous phase without visible Pb^0 precipitation. Fig. 8 illustrates the proposed biosorption pathway in *Enterococcus* sp., where ion exchange, EPS-mediated complexation, and electrostatic interactions dominate. This supports biosorption as the primary route Pb^{2+}removal in this system, highlighting its rapid and versatile nature compared to bioprecipitation.

4. Conclusion

This study highlights the bioremediation potential of *Enterococcus* sp. for selenite and lead, demonstrating that carbon source selection strongly influences removal efficiencies and mechanisms, with SeO_3^{2-} reduced through bioprecipitation and Pb^{2+} removed primarily via biosorption. By showing that biosurfactants promote SeO_3^{2-} precipitation and nanoparticle stabilisation but do not facilitate Pb^{2+} removal, our findings directly address the knowledge gap identified in the literature on the underexplored role of biosurfactants in metal and non-metal bioreduction. These insights not only strengthen mechanistic understanding but also inform future applications. Further research should focus on characterising the specific biosurfactant compounds and enzymatic pathways involved in Se reduction. Pilot-scale studies are also needed to evaluate *Enterococcus* sp. under real wastewater conditions. Finally, strategies should be developed for the recovery and valorisation of nano-Se for use in agriculture, medicine, and electronics.

CRediT authorship contribution statement

Job T. Tendenedzai: Writing – original draft, Methodology, Investigation, Data curation, Conceptualization. **Evans M.N. Chirwa:** Supervision, Funding acquisition, Resources, Writing – review & editing. **Hendrik G. Brink:** Writing – review & editing, Supervision, Resources, Funding acquisition, Conceptualization, Methodology.

Declaration of competing interest

The authors declare that they have no known competing financial interests or personal relationships that could have appeared to influence the work reported in this paper.

References

Abiodun, A.S., Ndanusa, A.J., Peter, A.O., 2019. Production of biosurfactants using Pseudomonas Aeruginosa for biodegradation of herbicide. Int. J. Biotechnol. 8 (1), 66–74. https://doi.org/10.18488/journal.57.2019.81.66.74.

Aslam, R., Mobin, M., Zehra, S., Aslam, J., 2023. Biosurfactants: types, sources, and production. In: Aslam, R., Mobin, M., Aslam, J., Zehra, S. (Eds.), Advancements in Biosurfactants Research. Springer International Publishing, Cham, pp. 3–24.

Ayangbenro, A.S., Babalola, O.O., 2017. A new strategy for heavy metal polluted environments: a review of microbial biosorbents. Int. J. Environ. Res. Public Health 14 (1). https://doi.org/10.3390/ijerph14010094.

Borah, S., Goswami, L., Sen, S., Sachan, D., Sarma, H., Montes, M., Peralta-Videa, J., Pakshirajan, K., Narayan, M., 2021. Selenite bioreduction and biosynthesis of selenium nanoparticles by Bacillus paramycoides SP3 isolated from coal mine overburden leachate. Environ. Pollut. 285, 117519. https://doi.org/10.1016/j.envpol.2021.117519.

Bradford, M.M., 1976. A rapid and sensitive method for the quantitation of microgram quantities of protein utilizing the principle of protein-dye binding. Anal. Biochem. 72 (1), 248–254. https://doi.org/10.1016/0003-2697(76)90527-3.

Brink, H.G., Wessels, C.E., Chirwa, E.M.N., 2018. Pseudomonas Stutzeri NT-I: optimal conditions for growth and selenate reduction. Chem. Eng. Trans. 70, 1651–1656. https://doi.org/10.3303/CET1870276.

Brozmanova, J., Manikova, D., Vlckova, V., Chovanec, M., 2010. Selenium: a double-edged sword for defense and offence in cancer. Arch. Toxicol. 84 (12), 919–938. https://doi.org/10.1007/s00204-010-0595-8.

Chaurasia, L.K., Tirwa, R.K., Tamang, B., 2022. Potential of Enterococcus faecium LM5. 2 for lipopeptide biosurfactant production and its effect on the growth of maize (Zea mays L.). Arch. Microbiol. 204 (4), 223. https://doi.org/10.1007/s00203-022-02834-9.

Chirwa, E.N.M., Mampholo, C.T., Fayemiwo, O.M., Bezza, F.A., 2017. Biosurfactant assisted recovery of the C5-C11 hydrocarbon fraction from oily sludge using biosurfactant producing consortium culture of bacteria. J. Environ. Manage 196, 261–269. https://doi.org/10.1016/j.jenvman.2017.03.011.

Chowdhury, I.R., Chowdhury, S., Mazumder, M.A.J., Al-Ahmed, A., 2022. Removal of lead ions (Pb2+) from water and wastewater: a review on the low-cost adsorbents. Appl. Water. Sci. 12 (8), 185. https://doi.org/10.1007/s13201-022-01703-6.

Cilliers, C., Brink, H., Chirwa, E., 2020. Pb(II) bio-removal, viability, and population distribution of an industrial microbial consortium: the effect of Pb(II) and nutrient concentrations. Sustainability 12, 2511. https://doi.org/10.3390/su12062511.

Cilliers, C., Neveling, O., Tichapondwa, S.M., Chirwa, E.M.N., Brink, H.G., 2022. Microbial Pb(II)-bioprecipitation: characterising responsible biotransformation mechanisms. J. Clean. Prod. 374, 133973. https://doi.org/10.1016/j.jclepro.2022.133973.

da Silva, R.R., da Silva, Y.A., de Lima e Silva, T.A., Sarubbo, L.A., de Luna, J.M., 2023. Biosurfactants as an eco-friendly technology in heavy metal remediation. In: Aslam, R., Mobin, M., Aslam, J., Zehra, S. (Eds.), Advancements in Biosurfactants Research. Springer International Publishing, Cham, pp. 225–235.

Essghaier, B., Mallat, N., Khwaldia, K., Mottola, F., Rocco, L., Hannachi, H., 2023. Production and characterization of new biosurfactants/bioemulsifiers from Pantoea alhagi and their antioxidant, antimicrobial and anti-biofilm potentiality evaluations. Molecules 28 (4), 1912. https://doi.org/10.3390/molecules28041912.

Fomina, M., Gadd, G.M., 2014. Biosorption: current perspectives on concept, definition and application. Bioresour. Technol. 160, 3–14. https://doi.org/10.1016/j.biortech.2013.12.102.

Gabr, R., Hassan, S., Shoreit, A., 2008. Biosorption of lead and nickel by living and non-living cells of Pseudomonas aeruginosa ASU 6a. Int. Biodeterior. Biodegradat. 62 (2), 195–203.
García-Solache, M., Rice, L.B., 2019. The Enterococcus: a model of adaptability to its environment. Clin. Microbiol. Rev. 32 (2). https://doi.org/10.1128/CMR.00058-18 e00058-00018.
Gayathiri, E., Prakash, P., Pratheep, T., Ramasubburayan, R., Thirumalaivasan, N., Gaur, A., Govindasamy, R., Rengasamy, K.R.R., 2024. Bio surfactants from lactic acid bacteria: an in-depth analysis of therapeutic properties and food formulation. Crit. Rev. Food Sci. Nutr. 64 (30), 10925–10949. https://doi.org/10.1080/10408398.2023.2230491.
Georgeson, L., Maslin, M., 2018. Putting the United Nations Sustainable Development Goals into practice: a review of implementation, monitoring, and finance. Geo: Geogr. Environ. 5 (1), e00049. https://doi.org/10.1002/geo2.49.
Gidudu, B., Chirwa, E., 2022. Evaluation of the toxicity of a rhamnolipid biosurfactant for its application in the optimization of the bio-electrokinetic remediation of petrochemical contaminated soil. Clean. Eng. Technol., 100521 https://doi.org/10.1016/j.clet.2022.100521.
Gupta, P., Diwan, B., 2017. Bacterial exopolysaccharide mediated heavy metal removal: a review on biosynthesis, mechanism and remediation strategies. Biotechnol. Rep. 13, 58–71. https://doi.org/10.1016/j.btre.2016.12.006.
Hassan, S., Awad, Y., Kabir, M., Oh, S.-E., Joo, J., 2010. Bacterial biosorption of heavy metals, pp. 79–110.
Huang, T., Liu, L., Zhang, S., Xu, J., 2019. Evaluation of electrokinetics coupled with a reactive barrier of activated carbon loaded with a nanoscale zero-valent iron for selenite removal from contaminated soils. J. Hazard. Mater. 368, 104–114. https://doi.org/10.1016/j.jhazmat.2019.01.036.
Jia, H., Huang, S., Cheng, S., Zhang, X., Chen, X., Zhang, Y., Wang, J., Wu, L., 2022. Novel mechanisms of selenite reduction in Bacillus subtilis 168:confirmation of multiple-pathway mediated remediation based on transcriptome analysis. J. Hazard. Mater. 433, 128834. https://doi.org/10.1016/j.jhazmat.2022.128834.
Joshi, S.J., Al-Wahaibi, Y.M., Al-Bahry, S.N., Elshafie, A.E., Al-Bemani, A.S., Al-Bahri, A., Al-Mandhari, M.S., 2016. Production, characterization, and application of Bacillus licheniformis W16 biosurfactant in enhancing oil recovery. Front. Microbiol. 7. https://doi.org/10.3389/fmicb.2016.01853.
Kachienga, L., 2020. The use of biosurfactants in the bioremediation of oil spills in water. In: Abia, A.L.K., Lanza, G.R. (Eds.), Current Microbiological Research in Africa: Selected Applications For Sustainable Environmental Management. Springer International Publishing, Cham, pp. 333–350.
Kagami, T., Narita, T., Kuroda, M., Notaguchi, E., Yamashita, M., Sei, K., Soda, S., Ike, M., 2013. Effective selenium volatilization under aerobic conditions and recovery from the aqueous phase by Pseudomonas stutzeri NT-I. Water. Res. 47 (3), 1361–1368. https://doi.org/10.1016/j.watres.2012.12.001.
Kamnev, A.A., Sadovnikova, J.N., Tarantilis, P.A., Polissiou, M.G., Antonyuk, L.P., 2008. Responses of azospirillum brasilense to nitrogen deficiency and to wheat Lectin: a diffuse reflectance infrared fourier transform (DRIFT) spectroscopic study. Microb. Ecol. 56 (4), 615–624. https://doi.org/10.1007/s00248-008-9381-z.
Kessi, J., Ramuz, M., Wehrli, E., Spycher, M., Bachofen, R., 1999. Reduction of selenite and detoxification of elemental selenium by the phototrophic bacterium rhodospirillum rubrum. Appl. Environ. Microbiol. 65 (11), 4734–4740. https://www.ncbi.nlm.nih.gov/pubmed/10543779.
Korayem, A., Abdelhafez, A., Zaki, M., Saleh, E., 2015. Optimization of biosurfactant production by streptomyces isolated from Egyptian arid soil using Plackett–Burman design. Annal. Agricult. Sci. 60 (2), 209–217. https://doi.org/10.1016/j.aoas.2015.09.001.
Lodeiro, P., Barriada, J.L., Herrero, R., Sastre de Vicente, M.E., 2007. Electrostatic effects in biosorption. The role of the electrochemistry. Portugaliae Electrochimica Acta 25 (1), 43–54 num2007.
Long, J, Yu, M, Xu, H, Huang, S, Wang, Z, Zhang, X-X, 2021. Characterization of cadmium biosorption by inactive biomass of two cadmium-tolerant endophytic bacteria Microbacterium sp. D2-2 and Bacillus sp. C9-3. Ecotoxicology 30 (7), 1419–1428. https://doi.org/10.1007/s10646-021-02363-z.
Mehdi, Y., Hornick, J.L., Istasse, L., Dufrasne, I., 2013. Selenium in the environment, metabolism and involvement in body functions. Molecules 18 (3), 3292–3311. https://doi.org/10.3390/molecules18033292.
Melati, R.B., Shimizu, F.L., Oliveira, G., Pagnocca, F.C., de Souza, W., Sant'Anna, C., Brienzo, M., 2019. Key factors affecting the recalcitrance and conversion process of Biomass. Bioenergy Res. 12 (1), 1–20. https://doi.org/10.1007/s12155-018-9941-0.
Mouafi, F.E., Elsoud, M.M.A., Moharam, M.E., 2016. Optimization of biosurfactant production by *Bacillus brevis* using response surface methodology. Biotechnol. Rep. 9, 31–37. https://doi.org/10.1016/j.btre.2015.12.003.
Mulligan, C.N., 2021. Sustainable remediation of contaminated soil using biosurfactants. Front. Bioeng. Biotechnol. 9. https://doi.org/10.3389/fbioe.2021.635196.
Naik, M.M., Dubey, S.K., 2013. Lead resistant bacteria: lead resistance mechanisms, their applications in lead bioremediation and biomonitoring. Ecotoxicol. Environ. Saf. 98, 1–7. https://doi.org/10.1016/j.ecoenv.2013.09.039.
Nancharaiah, Y.V., Lens, P.N.L., 2015. Selenium biomineralization for biotechnological applications. Trend. Biotechnol. 33 (6), 323–330. https://doi.org/10.1016/j.tibtech.2015.03.004.
Nikolova, C., Gutierrez, T., 2021. Biosurfactants and their applications in the oil and gas industry: current State of knowledge and future perspectives. Front. Bioeng. Biotechnol. 9. https://doi.org/10.3389/fbioe.2021.626639.
Ozyurek, S.B., Bilkay, I.S., 2017. Determination of petroleum biodegradation by bacteria isolated from drilling fluid, waste mud pit and crude oil. Turk. J. Biochem. 42 (6), 609–616. https://doi.org/10.1515/tjb-2017-0087.
Piacenza, E., Presentato, A., Ferrante, F., Cavallaro, G., Alduina, R., Chillura Martino, D. F., 2021. Biogenic selenium nanoparticles: a fine characterization to unveil their thermodynamic stability. Nanomaterials 11 (5), 1195. https://doi.org/10.3390/nano11051195.
Pratush, A., Kumar, A., Hu, Z., 2018. Adverse effect of heavy metals (As, Pb, Hg, and Cr) on health and their bioremediation strategies: a review. Int. Microbiol. 21 (3), 97–106. https://doi.org/10.1007/s10123-018-0012-3.
M.I. Rizvi, H., Verma, J.S., Ashish, 2021. Biosurfactants for oil pollution remediation. In: Inamuddin, Ahamed, Prasad, R. (Eds.), Microbial Biosurfactants: Preparation, Properties and Applications. Springer Singapore, Singapore, pp. 197–212. M.I.
Sajadi, S., 2010. Metal ion-binding properties of L-glutamic acid and L-aspartic acid, a comparative investigation. Nat. Sci. (Irvine) 2 (02), 85.
Shahabadi, N., Zendehcheshm, S., Mahdavi, M., 2023. Synthesis of Se nanoclusters via Ostwald ripening process: in vitro antibacterial and antioxidant activity. Emergent. Mater. 6. https://doi.org/10.1007/s42247-023-00455-6.
Sharma, D., Saharan, B.S., Chauhan, N., Procha, S., Lal, S., 2015. Isolation and functional characterization of novel biosurfactant produced by Enterococcus faecium. Springerplus. 4 (1), 4. https://doi.org/10.1186/2193-1801-4-4.
Sharma, N., Lavania, M., Lal, B., 2022. Biosurfactant: a next-generation tool for sustainable remediation of organic pollutants. Front. Microbiol. 12. https://doi.org/10.3389/fmicb.2021.821531.
Shoeibi, S., Mashreghi, M., 2017. Biosynthesis of selenium nanoparticles using Enterococcus faecalis and evaluation of their antibacterial activities. J. Trace Elem. Med. Biol. 39, 135–139. https://doi.org/10.1016/j.jtemb.2016.09.003.
Silva, M.E.T., Duvoisin Jr, S., Oliveira, R.L., Banhos, E.F., Souza, A.Q.L., Albuquerque, P. M., 2021. Biosurfactant production of Piper hispidum endophytic fungi. J. Appl. Microbiol. 130 (2), 561–569. https://doi.org/10.1111/jam.14398.
Sreedevi, P.R., Suresh, K., Jiang, G., 2022. Bacterial bioremediation of heavy metals in wastewater: a review of processes and applications. J. Water. Process. Eng. 48, 102884. https://doi.org/10.1016/j.jwpe.2022.102884.
Sun, F., Yan, Y., Liao, H., Bai, Y., Xing, B., Wu, F., 2014. Biosorption of antimony(V) by freshwater cyanobacteria microcystis from Lake Taihu, China: effects of pH and competitive ions. Environ. Sci. Pollut. Res. 21 (9), 5836–5848. https://doi.org/10.1007/s11356-014-2522-7.
Tendenedzai, J.T., Chirwa, E.M.N., Brink, H.G., 2021. Performance evaluation of selenite (SeO_3^{2-}) reduction by Enterococcus spp. Catalysts 11 (9), 1024. https://doi.org/10.3390/catal11091024.
Tendenedzai, J.T., Chirwa, E.M.N., Brink, H.G., spp, Enterococcus, 2022. Cell-Free extract: an abiotic route for synthesis of selenium nanoparticles (SeNPs), their characterisation and inhibition of *Escherichia coli*. Nanomaterials 12 (4), 658. https://doi.org/10.3390/nano12040658.
Tendenedzai, J.T., Chirwa, E.M.N., Brink, H.G., 2023. Kinetic modelling of selenite reduction by Enterococcus spp in batch reactors. Chem. Eng. Trans. 99, 13–18. https://doi.org/10.3303/CET2399003.
Torres, E., 2020. Biosorption: a review of the latest advances. Processes 8 (12), 1584. https://doi.org/10.3390/pr8121584.
Tugarova, A.V., Mamchenkova, P.V., Dyatlova, Y.A., Kamnev, A.A., 2018. FTIR and raman spectroscopic studies of selenium nanoparticles synthesised by the bacterium azospirillum thiophilum. Spectrochim. Acta Part A: Molecul. Biomolecul. Spectrosc. 192, 458–463. https://doi.org/10.1016/j.saa.2017.11.050.
Tugarova, A.V., Mamchenkova, P.V., Khanadeev, V.A., Kamnev, A.A., 2020. Selenite reduction by the rhizobacterium azospirillum brasilense, synthesis of extracellular selenium nanoparticles and their characterisation. N. Biotechnol. 58, 17–24. https://doi.org/10.1016/j.nbt.2020.02.003.
Van Khanh Nguyen, Younghyun, Park, J.Y., Lee, T., 2016. Microbial selenite reduction with organic carbon and electrode as sole electron donor by a bacterium isolated from domestic wastewater. Bioresour. Technol. 212, 182–189, 2016, **212**, 182-189.
Wang, Y., Ye, Q., Sun, Y., Jiang, Y., Meng, B., Du, J., Chen, J., Tugarova, A.V., Kamnev, A.A., Huang, S., 2022a. Selenite reduction by Proteus sp. YS02: new insights revealed by comparative transcriptomics and antibacterial effectiveness of the biogenic Se(0). Nanoparticl. Front. Microbiol. 13, 845321. https://doi.org/10.3389/fmicb.2022.845321.
Wang, Z., Wang, Y., Gomes, R.L., Gomes, H.I., 2022b. Selenium (Se) recovery for technological applications from environmental matrices based on biotic and abiotic mechanisms. J. Hazard. Mater. 427, 128122. https://doi.org/10.1016/j.jhazmat.2021.128122.
Yadav, P., Pandey, S., Dubey, S.K., 2023. Selenite bioreduction with concomitant green synthesis of selenium nanoparticles by a selenite resistant EPS and siderophore producing terrestrial bacterium. Biometals 36 (5), 1027–1045. https://doi.org/10.1007/s10534-023-00503-y.
Zheng, S., Su, J., Wang, L., Yao, R., Wang, D., Deng, Y., Wang, R., Wang, G., Rensing, C., 2014. Selenite reduction by the obligate aerobic bacterium Comamonas testosteroni S44 isolated from a metal-contaminated soil. BMC Microbiol. 14 (1), 204. https://doi.org/10.1186/s12866-014-0204-8.